Electromagnetic properties of polymer composites $Li_{0.33}Fe_{2.29}Zn_{0.21}Mn_{0.17}O_4$/P(VDF-TFE) in the frequency range 100−7000 MHz

© I.M. Isaev, V.G. Kostishin¶, R.I. Shakirzyanov, A.R. Kayumova, D.V. Salogub

National University of Science and Technology „MISiS“,
119049 Moscow, Russia

¶ E-mail: drvgkostishyn@mail.ru

Received August 19, 2021
Revised September 9, 2021
Accepted September 9, 2021

The article describes electromagnetic and microwave properties of the polymer composite with the lithium spinel ferrite inclusion of composition $Li_{0.33}Fe_{2.29}Zn_{0.21}Mn_{0.17}O_4$ in the frequency range 100−7000 MHz. It is shown that samples with a mass fraction of ferrite 60, 80% have pronounced radio-absorbing properties, measured using the reflection coefficient on a metal plate (return losses). For a composite with 80% ferrite, the minimum return loss was −37.5 dB at 2.71 GHz with an absorption width at −10 dB of 3 GHz. High absorption characteristics are directly related to the use of ferroelectric polymer P(VDF-TFE) as a binder, which is expressed in the combined action of the absorption mechanisms of the magnetic and ferroelectric phases.

Keywords: lithium ferrite, polymer composite, polyvinylidene fluoride, radio-absorbing material.

DOI: 10.21883/SC.2022.01.53026.9728

1. Introduction

Ferrites $Me_xFe_{2-x}O_4$ with spinel structure are well-known magnetic semiconductors. These materials are actively studied by researchers all over the world due to high potential for variation of their physical properties. By introducing the isomorphous substitutions it is possible to change saturation magnetization, coercitive force, electrical conductivity, magnetostriction constant, magnetic losses, catalytic, magnetocaloric and other properties [1,2]. This results in rather impressive list of ferrospinel applications and research trends in biomedicine and medical diagnostics [3], as components of microwave devices (circulators, valves), electronic devices, magnetoelectronics (magnetic semiconductors) [4,5], gas sensors [6], electronic components and electrical circuit components, radiation absorbing materials and even in water treatment technologies [7]. Currently, the large variety of methods for ferrites production are developed, but one of the widely used is still the method of ceramic processing technology due to its high producibility and utilization in industry. Since there is an acute problem related with electromagnetic compatibility and electromagnetic pollution, the works are performed on creation of technologies of electromagnetic shielding or electromagnetic radiation level suppression [8]. Ferrites and polymeric composites based on them are great to use as radiation absorbing materials, since they are materials with pronounced magnetic properties with high or medium resistivity [9–12]. The latter is especially important since conductors usually have high value of reflection coefficient, that complicates the use as radiation absorbing materials. Researchers are very interested in ferrite spinels doped with Li, since lithium spinels can have high values of saturation magnetization [13,14] due to irregular distribution of cations over sub-lattices, cut-off frequency of ~ 500 MHz [15], low values of sintering temperature of 880−920°C [16], values of electric conductivity with direct current of $\sim 10^{-12}-10^{-5}\,\mathrm{Ohm}^{-1}\cdot\mathrm{cm}^{-1}$, dielectric losses in a wide range of frequencies [17], low width of resonance line of 1−10 Oe [18].

Earlier in [19] it was shown that Li-Mn-Zn ferrite with chemical composition of $Li_{0.33}Fe_{2.29}Zn_{0.21}Mn_{0.17}O_4$ is characterized as radiation absorbing material within frequency range of 0.05−7 GHz. Coefficient of reflection on a metal plate for samples with sintering temperature of 1050−1100°C was −22.52 dB at frequency of 1.34 GHz. It was shown that one of the minimums of the reflection coefficient coincides with natural ferromagnetic resonance in terms of frequency position. Also there were no dielectric losses within the examined frequency range for ferrite $Li_{0.33}Fe_{2.29}Zn_{0.21}Mn_{0.17}O_4$. The conclusion was made that the electromagnetic losses in Li-Mn-Zn ferrite were caused by magnetic losses due to domain-wall resonance (DWR) and natural ferromagnetic resonance (NFMR). This study is focused on examination of radiation absorbing properties of composites of poly(vinylidenfluoride-tetrafluoroethylene)/Li-Mn-Zn ferrite. Choice of electrically active PVDF copolymer is caused by presence of ferroelectric phase in it, that can make an additional contribution to high-frequency losses of electromagnetic energy due to repolarization processes.

2. Experimental part

Copolymer of polyvinylidenfluoride (F2M brand) $-[(CF_2\text{-}CH_2)_n\text{-}(CF_2\text{-}CF_2)_m]_k-$ with ratio of monomers in

circuit of $n = 96$, $m = 4$ and ferrite-spinel with chemical composition of $Li_{0.33}Fe_{2.29}Zn_{0.21}Mn_{0.17}O_4$ were used as initial materials. Ferrite ceramics production was described earlier in study [19]. Powder size was $< 45\,\mu$m, that allowed to obtain the homogeneous mechanical mixture in a mortar. Mixture homogeneity was indirectly evaluated with color change. Then, the mixture was put into a mold with heater, which were put under hydraulic press. Heating was performed at constant pressure of ~ 12 MPa to temperature of 190°C. At this temperature the exposure was performed for 10 min, after which the mold was cooled on air to room temperature. Samples were produced of a ring-shape with outer diameter of 16 mm, inner diameter of 7 mm and height of 6 mm. The sample of ceramic sintered ferrite product of similar composition and sizes was also used for electrophysical characteristics comparison. Diffractograms were made using X-ray diffractometer Difrei ($CrK_\alpha radiation$). Lattice parameter was defined using the formula for cubic crystal:

$$\frac{1}{d(hkl)} = \frac{h^2 + k^2 + l^2}{a^2}, \qquad (1)$$

where d is the interplanar distance of reflex (hkl), a is the lattice parameter.

Crystallites size was evaluated using the Scherrer equation:

$$D = \frac{\lambda}{\beta \cos\theta}, \qquad (2)$$

where β is the width on the reflex half-height.

Micrographs of scanning electron microscopy were made using the electron microscope ThermoFisher Apreo. Electromagnetic spectra (complex dielectric permeability, complex magnetic permeability) were measured using coaxial cell and vector network analyzer Rohde & Shwartz ZVL-13.

3. Results and discussion

X-ray phase analysis of initial powders and composites shows that during thermal pressing process the external phases are not formed (Fig. 1). In initial ferrite powder the phase α-Fe_2O_3 content was observed. Phase analysis was performed using Match!3 software. For that purpose we used diffraction maps of COD base № 96-153-3269 ($Li_{0.25}Zn_{0.5}Fe_{2.25}O_4$, spinel phase) and № 96-900-0140 (Fe_2O_3, hematite phase). Determination of the lattice parameter for ferrite powder using the formula (1) gives the value for spinel elementary cell 8.3344 Å, and average size of crystallite D using the formula (2) is 36.91 nm. For sintered ferrite $a = 8.3601$ Å, $D = 108.8$ nm. X-ray structural analysis data can indicate the difference between ferrite powder microstructure and sintered ferrite microstructure: ferrite powder generally has the smaller grain size (and crystallites size) compared to the sintered ferrite ceramics, that correlates with the results of studies [20,21]. As will be shown further, this fact can significantly influence on the spectra type of the electromagnetic characteristics of

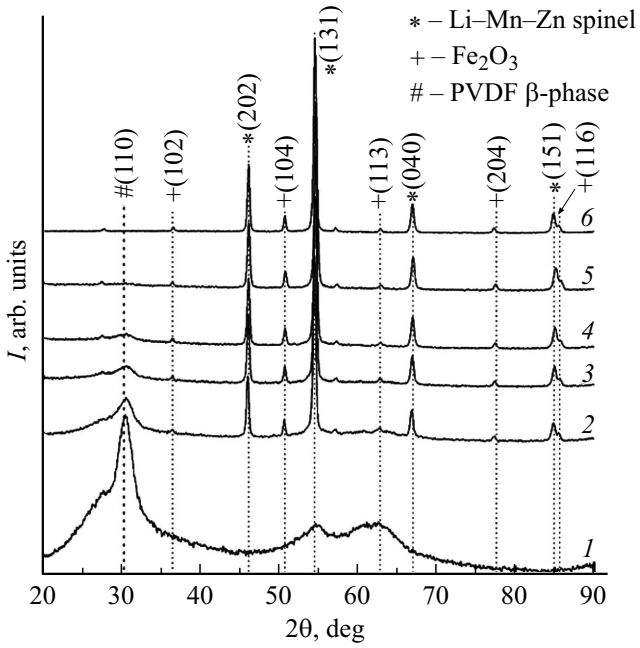

Figure 1. Diffractograms of X-ray phase analysis (XPA) of initial components and composites: *1* — P(VDF-TFE); *2* — composite with mass fraction of 20%, *3* — composite with mass fraction of 40%, *4* — composite with mass fraction of 60%, *5* — composite with mass fraction of 80%; *6* — powder of Li-Mn-Zn-ferrite.

the samples of fine powder and sintered product. It also should be noted that PVDF copolymer reflex decomposition into components, related to the ordered ferroelectric β-phase (110) and paraelectric phase, shows that with introduction of ferrite mass fraction, equal to 20%, the increase of crystallite size in the composite from 7.28 to 10.82 nm is observed. This can indicate the rise of polymer crystallinity degree at introduction of ferrite inclusions, as was described in other studies on composites of ferrite-spinel/PVDF [22,23].

Figures 2, *a* and 2, *b* show spectra of complex magnetic permeability of the examined samples. Spectra of magnetic permeability of ceramic ferrite product show two distinct areas with $\mu'(f)$ bend, while $\mu''(f)$ dependence goes through the maximum. This fact can be explained with different frequencies of NFMR and DWR in $Li_{0.33}Fe_{2.29}Zn_{0.21}Mn_{0.17}O_4$ ferrite. Maximum μ'' on the frequency corresponds to spin rotation process or NFMR, while maximum on the frequency of 0.04 GHz — to DWR. In composites based on Li-Mn-Zn ferrite the contribution of DWR is significantly reduced, since the particles are too small to contain large amount of domains. It indirectly indicates the reduction of crystallites size D, since with grain size reduction the contribution of magnetization rotation in magnetic domains will be lower. Domain walls quantity decreases and low-frequency value of μ'' also decreases. As per Kramers-Kronig relation, with decrease of values of the imaginary part of the complex value the real part also decreases. Therefore, the real part of the magnetic

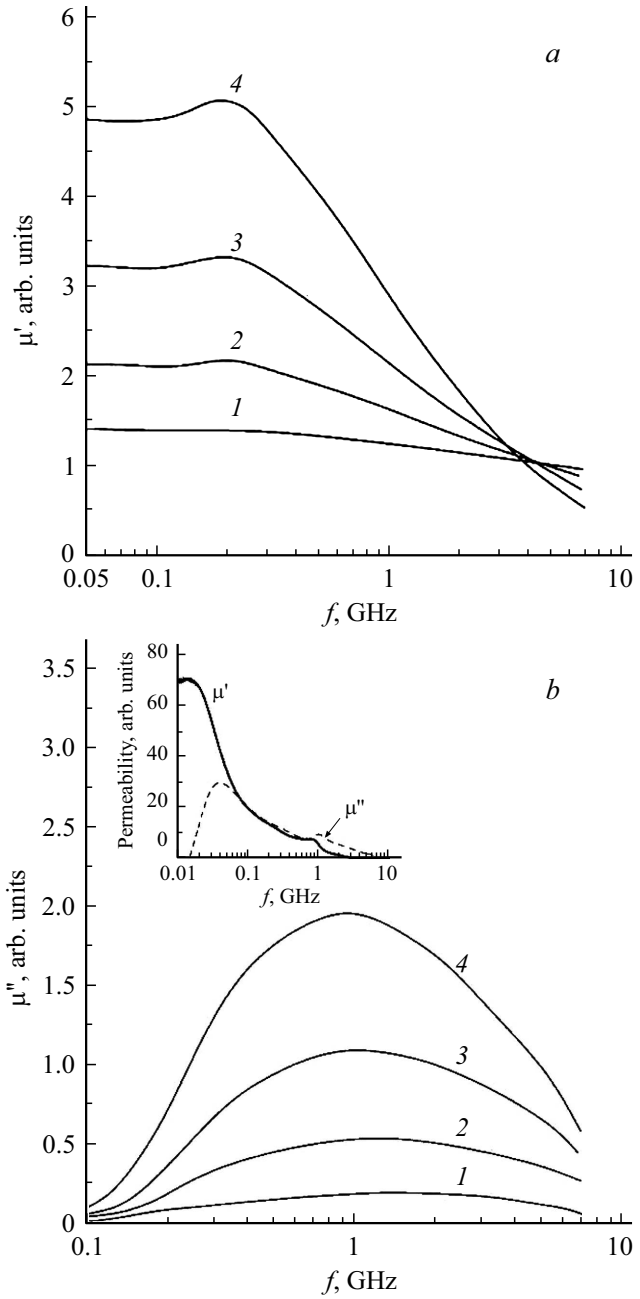

Figure 2. *a* — spectra of real part of magnetic permeability of composites of P(VDF-TFE)/$Li_{0.33}Fe_{2.29}Zn_{0.21}Mn_{0.17}O_4$ with various mass fraction of ferrite. *b* — spectra of imaginary part of magnetic permeability of composites of P(VDF-TFE)/$Li_{0.33}Fe_{2.29}Zn_{0.21}Mn_{0.17}O_4$ with various mass fraction of ferrite. On insert — spectrum of ceramic product $Li_{0.33}Fe_{2.29}Zn_{0.21}Mn_{0.17}O_4$, %: *1* — 20, *2* — 40, *3* — 60, *4* — 80.

permeability also significantly decreases. On the other side, reduction of the conservative part of the magnetic permeability μ' is related to magnetic induction decrease inside the material due to presence of non-magnetic polymeric layers. It also can be noted that the frequency position of maximum μ'' in composites is shifted towards the area of high frequencies with polymer concentration increase. Thus, for 60 and 80% of composites the position of $\mu''_{\max}$ is ~ 0.95 GHz, while for 40 and 20% — 1.23 and 1.49 GHz, respectively. Shifting of dependence maximum $\mu''(f)$ is happened with variation of internal magnetic field inside the composite. As was described earlier, contribution of DWR to $\mu''(f)$ spectrum is rather small. Therefore, the spectrum type is defined with NFMR process. In case of non-magnetic layers between ferrite particles the additional fields of internal demagnetizing factors, that can change the value of the internal field H_{eff} [24], appear. While the calculation of internal field inside the composite is a complicated task, that requires its own study, in case of spectra examined in this study we can assert that, considering that NFMR resonance frequency in ferrite is defined with relation $f_r = \gamma H_{\text{eff}}$, the internal field increases, since NFMR frequency in the less concentrated composite is maximum.

Figure 3 shows the spectra of the real part of dielectric permittivity. With increases of ferrite concentration the ε' of the composites also increase, that correlates with theoretical models of effective medium, in which the effective dielectric permeability of heterogeneous medium is a function of permeabilities of individual components [25]. Such statement is correct, since, as shown in the figure, dielectric permeability of F2M polymer is ~ 3.5, and of Li-Mn-Zn ferrite is ~ 6. Almost identical value of dielectric permeability of the composite with mass fraction of 80% of magnetic inclusions and the sintered product of $Li_{0.33}Fe_{2.29}Zn_{0.21}Mn_{0.17}O_4$ should be noted. This fact can be explained, bearing in mind that at this concentration

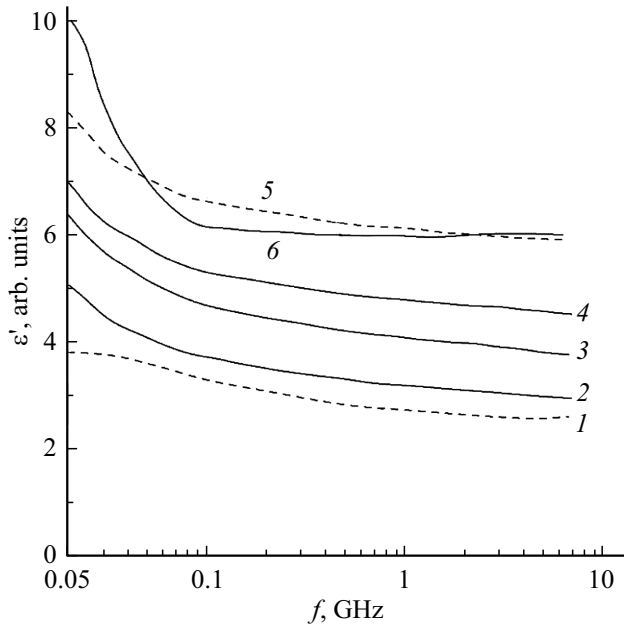

Figure 3. Dependencies of real part of dielectric permeability of the examined samples with various mass fraction of ferrite: *1* — P(VDF-TFE); *2* — 20, *3* — 40, *4* — 60, *5* — 80%; *6* — ceramic sample $Li_{0.33}Fe_{2.29}Zn_{0.21}Mn_{0.17}O_4$.

the matrix and filler change the positions, i.e. the layers of P(VDF-TFE) polymer are evenly distributed in ferrite matrix, while not all particles are incapsulated with polymer. It can be seen in images of scanning electron microscopy (Fig. 4), which show that individual particles of inclusions contact with each other and form clusters. In this case the electrical percolation is happened, due to which the passing high-frequency current goes solely through channels, created by ferrite particles. In this case the dielectric permittivity of the composite can be equal to ferrite permittivity. For spectra of the imaginary part of dielectric permeability ε'' it was observed that permittivity value does not depend on concentration of inclusions and slowly decreases from ~ 0.6 to ~ 0.18 in the frequency range of 100−7000 MHz.

Electromagnetic absorption properties absorption properties were evaluated as per spectra of coefficient of reflection on metal plate R_l, that was experimentally measured for rings with thickness of 6 mm on short-circuited cell (Fig. 5). Formulas of calculation of reflection coefficient R_l and normalized impedance Z_{in}/Z_0 were used for analysis of factors, resulting in high absorption:

$$R_l = 20 \log \left| \frac{Z_{\text{in}} - Z_0}{Z_{\text{in}} + Z_0} \right|, \tag{3}$$

$$\frac{Z_{\text{in}}}{Z_0} = \sqrt{\frac{\mu_r^*}{\varepsilon_r^*}} \tanh \left[j \frac{2\pi f h}{c} \sqrt{\mu_r^* \varepsilon_r^*} \right], \tag{4}$$

where Z_0 is the free space impedance, h is the absorbent thickness, c is the light velocity.

It was observed that composite with 60% of ferrite has the lowest reflection coefficient with minimum value $R_l = -35$ dB. It should also be noted that the observed spectrum is characterized with significantly high absorption width Δf on a level of 10 dB of about ~ 4 GHz. As seen from formulas (1), (2), the maximum absorption (minimum value of reflection coefficient) in geometry with perfect reflector behind absorbent is possible at equality of impedances Z_{in} and Z_0 (or $Z_{\text{in}}/Z_0 = 1$), that characterize the sample input impedance and free space impedance, respectively. If the normalized impedance is close to 1, the condition of ideal matching is met [26], at which the waves, reflected from air/absorbent interface and from metal plate, interfere with equal amplitudes. Peak position is also related to interference thickness, that can be calculated as per quarter-wave agreement model [27] using the equation:

$$t_{\lambda/4} = nc / \left(4 f_0 \sqrt{|\varepsilon^* \mu^*|}\right), \tag{5}$$

where n is the odd natural number 1, 3, 5 ..., f_0 is the frequency of electromagnetic radiation (EMR), c is the light velocity.

Equation (2) shows that the value of normalized impedance depends on values of complex magnetic and dielectric permeabilities. In this case the certain „set“ of values of real and imaginary parts of permeabilities can define the value $Z_{\text{in}}/Z_0 = 1$, and, consequently, the low reflection. Calculating diagrams for determination of ideal

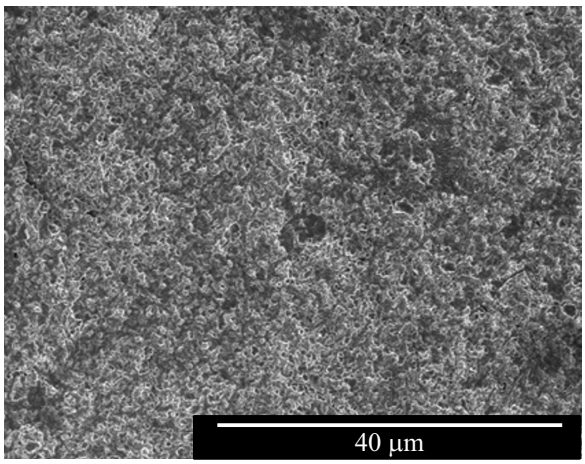

Figure 4. Micrograph of scanning electron microscopy of the composite with mass fraction of 80%.

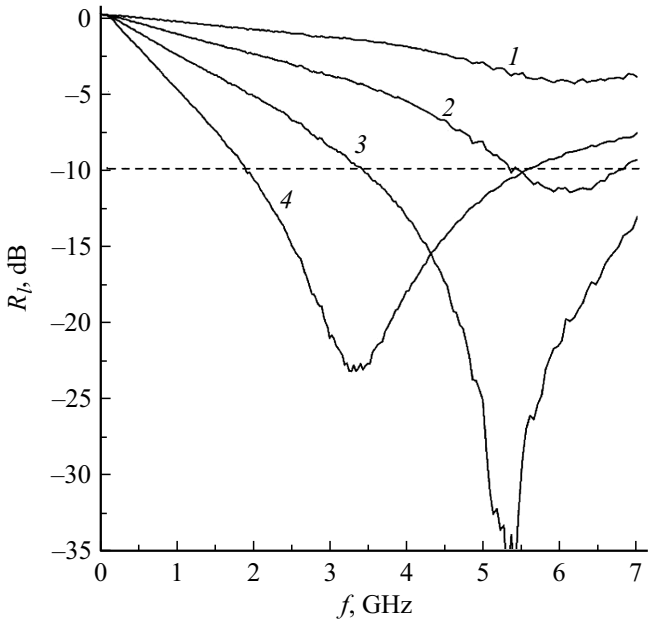

Figure 5. Spectra of reflection on metal plate of composites with thickness of 6 mm of the composition F2M-$Li_{0.33}Fe_{2.29}Zn_{0.21}Mn_{0.17}O_4$ with various mass fraction of ferrite, %: *1* — 20, *2* — 40, *3* — 60, *4* — 80.

matching conditions for radiation absorbing material (RAM) on a perfect reflector are presented, for instance, in [28]. Despite of such approach of radiation absorbing characteristics describing, it should be understood that „the lucky“ combination of permeability values is defined by the physical processes in materials. In case of the examined composites, this is the processes of dipoles repolarization in polymer, ferrite and resonance absorption of electromagnetic wave at magnetic torque rotation, magnetic domain walls movement. Moreover, their simultaneous action can result in synergetic effect, under which the electromagnetic waves (EMW) weakening significantly increases. Study [29] includes the

Comparison of absorption parameters of experimental and design spectra R_l

C_m, %	h, mm	f_0, GHz	$R_l^{\max}$, dB	Δf, GHz	Z_{in}/Z_0	$t_{\lambda/4}$, mm	$\tan\delta_\varepsilon$	$\tan\delta_\mu$
20	6*	6.18*	−4.5*	–	1.96	7	0.05	0.17
40	6*	6.13*	−11.6*	–	1.65	6.3	0.05	0.37
60	6*	5.37*	−33.8*	4.2*	1.02	6.3	0.05	0.74
60	7	4.26	−25.0	3.6	1.13	7.4	0.04	0.69
60	8	3.60	−21.9	2.8	1.18	8.3	0.04	0.69
80	5	4.49	−17.7	4.0	0.77	5.8	0.03	1.19
80	6*	3.35*	−23.2*	3.7*	0.88	6.9	0.04	1.12
80	7	2.71	−37.5	3.0	0.98	7.9	0.04	1.06
80	8	2.29	−30.1	2.4	1.07	8.8	0.04	0.99

Note. $R_l^{\max}$ is the peak value of reflection coefficient, f_0 is the peak frequency position, Δf is the absorption width on level of −10 dB, Z_{in}/Z_0 is the normalized impedance, $t_{\lambda/4}$ is the interference thickness. * is the experimental data.

results, indicating that composites based on electrically active PVDF matrix demonstrate higher electromagnetic energy weakening compared to matrices of linear dielectrics. Thus, the conclusion can be made that high absorption in concentrated composites can be related to ferroelectric behavior of the matrix (binder). However, if we consider the design values of tangents of magnetic $\tan\delta_\mu = \mu''/\mu'$, and dielectric losses $\tan\delta_\varepsilon = \varepsilon''/\varepsilon'$, the main contribution to electromagnetic energy losses in the resulting samples is made by magnetic losses, since the values of $\tan\delta_\mu$ are in large excess of dielectric losses tangent values. With magnetic phase increase the values of $\tan\delta_\mu$ and $|R_l|$ also increase. Summary data on analysis of radiation absorption factors are presented in the table. It can be noted that design values of $t_{\lambda/4}$ not always coincide with real or set thickness of absorbent. It can be related to reflection peak smearing, when the frequency f_0 is uncertainly defined. On the other side, in some studies it is noted that formula (5) gives only qualitative explanation and is not always compliant with experimental data.

4. Conclusion

Ferrite-polymeric composites of P(VDF-TFE)/$Li_{0.33}Fe_{2.29}Zn_{0.21}Mn_{0.17}O_4$, observed in the study, were made with mass fraction of ferrite of 20, 40, 60, 80%. It was shown that with ferrite concentration increase the values of complex dielectric and magnetic permeability also increase, while in case of magnetic permeability the dispersion shift towards the area of low frequencies was observed. Pronounced radiation absorbing properties, measured through spectra of coefficient of reflection on metal plate, were observed in composites with mass fraction of 60, 80%. For composite with mass fraction of 60% with thickness of 6 mm the minimum reflection coefficient was $R_l = -33.8$ dB at frequency $f_0 = 5.37$ GHz with absorption width on a level of −10 dB of about $\Delta f = 4$ GHz, and for composite with mass fraction of 80% the same parameters with thickness of 7 mm were −37.5 dB, 2.71 GHz, 3 GHz, respectively. It is shown that absorption in composites is caused by impedance matching, magnetic losses due to NFMR and DWR, and possible synergetic effect due to dielectric and magnetic losses from ferroelectric and magnetic phases.

Funding

This study was supported by a grant from the Russian Science Foundation (agreement No. 19-19-00694 dated 06.05.2019).

Conflict of interest

The authors declare that they have no conflict of interest.

References

[1] S.B. Narang, K. Pubby. J. Magn. Magn. Mater., **519**, 167163 (2021).
[2] P. Thakur, D. Chahar, S. Taneja, N. Bhalla, A. Thakur. Ceram. Int., **46** (10, pt B), 15740 (2020).
[3] K.K. Kefeni, T.A.M. Msagati, T.T. Nkambule, B.B. Mamba. Mater. Sci. Eng. C, **107**, 110314 (2020).
[4] L.M. Letyuk, V.G. Kostishin, A.V. Gonchar. Tekhnologiya ferritovykh materialov magnitoelektroniki (M., MISiS, 2005) p. 352 (in Russian).
[5] P.B. Belavi, G.N. Chavan, L.R. Naik, R. Somashekar, R.K. Kotnala. Mater. Chem. Phys., **132** (1), 138 (2012).
[6] V. Manikandan, J.H. Kim, A. Mirzaei, S.S. Kim, S. Vigneselvan, M. Singh, J. Chandrasekaran. J. Mol. Struct., **1177**, 485 (2019).
[7] S. Rana, J. Rawat, R.D.K. Misra. Acta Biomaterialia, **1** (6), 691 (2005).
[8] E.V. Yakushko, L.V. Kozhitov, D.G. Muratov, E.Y. Korovin, A.A. Lomov, A.V. Popkova. Rus. Phys. J., **63** (12), 2226 (2021).
[9] X. Zeng, X. Cheng, R. Yu, G.D. Stucky. Carbon, **168**, 606 (2020).
[10] N.N. Ali, Y. Atassi, A. Salloum, A. Charba, A. Malki, M. Jafarian. Mater. Chem. Phys., **211**, 79 (2018).
[11] Z. Jiao, Z. Yao, J. Zhou, K. Qian, Y. Lei, B. Wei, W. Chen. Ceram. Int., **46** (16, pt A), 25405 (2020).

[12] P. Saha, T. Debnath, S. Das, S. Chatterjee, S. Sutradhar. Mater. Sci. Eng. B, **245**, 17 (2019).
[13] M. Arana, P.G. Bercoff, S.E. Jacobo. Procedia Mater. Sci., **1**, 620 (2012).
[14] M. Arana, V. Galvan, S.E. Jacobo, P.G. Bercoff. J. Alloys Compd., **568**, 5 (2013).
[15] F. Xie, Y. Chen, M. Bai, P. Wang. Ceram. Int., **45** (14), 17915 (2019).
[16] X. Wang, Y. Li, Z. Chen, H. Zhang, H. Su, G. Wang, Y. Liao, Z. Zhong. J. Alloys Compd., **797**, 566 (2019).
[17] Y. Gao, Z. Wang, R. Shi, J. Pei, H. Zhang, X. Zhou. J. Alloys Compd., **805**, 934 (2019).
[18] P. Baba, G. Argentina, W. Courtney, G. Dionne, D. Temme. IEEE Trans. Magn., **8** (1), 83 (1972).
[19] I.M. Isaev, V.G. Kostishin, V.V. Korovushkin, D.V. Salogub, R.I. Shakirzyanov, A.V. Timofeev, A.Yu. Mironovich. Tech. Phys., **66** (9), 1344 (2021)
[20] T.Ungár, G. Tichy, J. Gubicza, R. Hellmig. Powder Diffr., 20 (4), 366 (2005).
[21] R. Singh Yadav, I. Kuřitka, J. Vilcakova, J. Havlica, J. Masilko, L. Kalina, J. Tkacz, J. Švec, V. Enev, M. Hajdúchová. Adv. Nat. Sci: Nanosci. Nanotechnol., **8**, 045002 (2017).
[22] R.I. Shakirzyanov, V.G. Kostishyn, A.T. Morchenko, I.M. Isaev, V.V. Kozlov, V.A. Astakhov. Russ. J. Inorg. Chem., **65** (6), 829 (2020). DOI 10.1134/S0036023620060194
[23] P. Martins, C.M. Costa, S. Lanceros-Mendez. Appl. Phys. A, **103**, 233 (2011).
[24] V. Babayan, N.E. Kazantseva, R. Moučka, I. Sapurina, Yu.M. Spivak, V.A. Moshnikov. J. Magn. Magn., **324** (2), 161 (2012).
[25] V.A. Astakhov, R.I. Shakirzyanov, A.T. Morchenko, Z.V. Mingazheva, S.P. Kurochka. J. Nano-Electron. Phys., **8** (3), 03044 (2016).
[26] B. Wang, J. Wei, L. Qiao, T. Wang, F. Li. J. Magn. Magn. Mater., **324**, 761 (2012).
[27] B. Wang, J. Wei, Y. Yang, T. Wang, F. Li. J. Magn. Magn. Mater., **323** (8), 1101 (2011).
[28] H.M. Musal, D.C. Smith. IEEE Trans. Magn., **26** (5), 1462 (1990).
[29] V.V. Kochervinskii. Bull. Rus. Acad. Sci., ser. phys., **84** (2), 144 (2020).